

Research Paper

Blocking TRPM4 alleviates pancreatic acinar cell damage via an NMDA receptor-dependent pathway in acute pancreatitis

Yifan Ren^{1,2*}; Qing Cui^{3*}; Wuming Liu^{1,4}; Hangcheng Liu²; Tao Wang^{1,4}; Hongwei Lu²; Yi Lv^{1,4}; Rongqian Wu¹

1. National Local Joint Engineering Research Center for Precision Surgery & Regenerative Medicine, Shaanxi Provincial Center for Regenerative Medicine and Surgical Engineering, First Affiliated Hospital of Xi'an Jiaotong University, Xi'an, Shaanxi Province, China.
2. Department of General Surgery, The Second Affiliated Hospital of Xi'an Jiaotong University, Xi'an, Shaanxi Province, China.
3. Department of Cardiology, Xi'an Third Hospital Affiliated to Northwest University, Xi'an, Shaanxi Province, China.
4. Department of Hepatobiliary Surgery, First Affiliated Hospital of Xi'an Jiaotong University, Xi'an, Shaanxi Province, China.

*These authors contributed equally to this work.

 Corresponding authors: Rongqian Wu and Yi Lv, MD, PhD, Professor, National-Local Joint Engineering Research Center for Precision Surgery & Regenerative Medicine, First Affiliated Hospital of Xi'an Jiaotong University, 76 West Yanta Road, P.O. Box 124, Xi'an, Shaanxi Province 710061, China. Email: Rongqian Wu: rwu001@mail.xjtu.edu.cn; Yi Lv: luyi169@mail.xjtu.edu.cn.

© The author(s). This is an open access article distributed under the terms of the Creative Commons Attribution License (<https://creativecommons.org/licenses/by/4.0/>). See <https://ivyspring.com/terms> for full terms and conditions.

Received: 2025.04.27; Accepted: 2025.05.28; Published: 2025.06.09

Abstract

Background: Mitochondrial dysfunction caused by Ca²⁺ overload in pancreatic acinar cells is an important mechanism in the pathogenesis of acute pancreatitis (AP). Transient receptor potential cation channel melastatin 4 (TRPM4), a non-selective cation channel, can be activated by intracellular Ca²⁺, and is involved in mediating damage to neuronal mitochondrial function. However, the role of TRPM4 activation in mitochondrial dysfunction during AP remains unknown.

Methods: We employed three mouse models of AP (intraperitoneal administration of L-arginine, cerulein plus lipopolysaccharides (LPS), or cerulein alone) for *in vivo* studies. For *in vitro* studies, cerulein+ LPS was used to induce mitochondrial dysfunction and cell death in AR42J cell. *Trpm4* gene-defective mice and plasmids were utilized to downregulate the expression of TRPM4 in mice or overexpress TRPM4 in AR42J. 9-Phenanthrol, a specific inhibitor of TRPM4, was used to antagonize TRPM4 activity both *in vitro* and *in vivo*.

Results: Pancreatic TRPM4 levels were increased in all three AP models. Blocking TRPM4 activity with 9-phenanthrol or knocking down TRPM4 expression alleviated pancreatic damage and reduced mortality in AP mice. The protective effect of TRPM4 defects on AP was associated with improved mitochondrial function in pancreatic acinar cells. Mechanistically, TRPM4 activation induced mitochondrial dysfunction and cell death in AP were dependent on the presence of N-methyl-D-aspartate receptors (NMDARs). Blocking NMDARs mitigates the aggravated mitochondrial damage, ER stress and cell death caused by TRPM4 activation in AP.

Conclusions: TRPM4 activation contributes to pancreatic acinar cells damage via an NMDAs-dependent pathway in AP. The TRPM4/NMDARs complex provides a new target for the future treatment of AP.

Keywords: acute pancreatitis; intracellular Ca²⁺; TRPM4/NMDARs; mitochondrial dysfunction; ER stress

Introduction

Acute pancreatitis (AP) is a disease characterized by the self-digestion of pancreatic tissue, accompanied by varying degrees of tissue destruction, edema or hemorrhage [1]. Alcohol, hyperlipidemia, and cholelithiasis account for approximately 72% of AP cases [2]. Severe AP is a non-self-limiting syndrome characterized by

pancreatic necrosis and a high risk of multiple organ dysfunction syndrome (MODS), placing a heavy burden on intensive care units [3]. Due to the limited understanding of its pathogenesis, palliative treatment is the main treatment for severe AP, and specific treatments are still elusive [4].

Healthy mitochondria play a core role in

maintaining the normal homeostasis of pancreatic exocrine acinar cells [5, 6]. Many studies have shown that abnormal mitochondrial function is a key factor in AP pathogenesis [7-9]. Mitochondrial damage caused by a variety of pathogenic factors can lead to impaired autophagy and subsequently cause lipid metabolism disorders and endoplasmic reticulum stress (ER stress) in AP [10]. Our previous studies have shown that impaired mitochondrial dynamics induces oxidative stress in pancreatic cell, aggravate the unfolded protein response (UPR), promote cell apoptosis and trigger an inflammatory response [11-13]. Therefore, restoring impaired mitochondrial function in AP provides a rationale for developing targeted therapeutic options.

Calcium (Ca^{2+}) overload is a key contributor to exocrine acinar cells injury in AP [14]. Transient receptor potential cation channel melastatin 4 (TRPM4) is a non-selective cation channel that can be activated by increasing the concentration of cytoplasmic Ca^{2+} [15-17]. TRPM4 activation causes mitochondrial injury and cell death in the nervous system when TRPM4 is physically coupled with N-methyl-d-aspartate receptors (NMDARs), a class of glutamate-gated, calcium-permeable neurotransmitter receptors [18]. Both NMDARs and TRPM4 are expressed in the pancreas. However, the role of TRPM4 activation and its interaction with NMDARs in pancreatic cell injury during AP remains unknown. Therefore, we hypothesized that TRPM4 activation leads to pancreatic cell damage via an NMDAs-dependent pathway in AP. The aim of this study was to determine whether pancreatic cell injury in AP is related to TRPM4 activation and, if so, the role of TRPM4 and NMDARs interactions in this process. We investigated whether TRPM4 is involved in the association between elevated intracellular Ca^{2+} levels and mitochondrial dysfunction. This study provides mechanistic insight for the development of targeted treatments for AP.

Results

TRPM4 expression is increased in various AP models

To elucidate the role of TRPM4 in AP, we first examined changes in TRPM4 expression levels in the pancreas. As shown in Figures 1A-B, L-arginine or Cerulein+ lipopolysaccharides (LPS) or Cerulein alone were used to induce different mouse AP models, respectively (Detailed description is given in the *Materials and Methods*). The expression level of TRPM4 in the mouse pancreas was almost unchanged within 48 h after the intraperitoneal injection of

L-arginine; however, it increased to approximately 1.5 times than the base level at 72 h ($P < 0.05$, Figure 1C). A significant increase in TRPM4 expression was observed in mice at 11 h after AP induction with cerulein+ LPS, and the TRPM4 level returned to the baseline level at 15 h ($P < 0.05$, Figure 1D). Furthermore, the expression trend of TRPM4 in cerulein- treated AP model mice was similar to that in cerulein+ LPS-induced AP model mice (Figure 1E), suggesting that the two models may share the same pathogenesis. Figure 1F shows the TRPM4 expression in the pancreatic tissue of AP model mice and control mice. The destruction of pancreatic tissue combined with the deepening of TRPM4 staining confirmed the conclusions obtained in Figures 1C-E.

9-phenanthrol protects against pancreatic injury in experimental AP

Pathological examination revealed the role of TRPM4 in AP development. As shown in Figures 2A-C & Figures S1A-C, L-arginine-, cerulein+ LPS-, cerulein-induced AP caused different degrees of pancreatic damage in mice. Among them, cerulein-induced AP was less severe than L-arginine- or cerulein+ LPS-induced AP. The intraperitoneal injection of the TRPM4 inhibitor 9-phenanthrol alleviated or eliminated pancreatic injury and necrosis in the three mouse models of AP. 9-phenanthrol exhibited a dose-dependent protective effect on the pancreas ($P < 0.05$, Figures 2A-C; $P > 0.05$, Figures S1A - C).

Severe AP is often accompanied by pancreatic hemorrhage, necrosis, and macroscopic reductions in pancreatic volume and weight. Mild AP, also known as edematous pancreatitis, is associated with or without weight gain due to congestive edema of the pancreas [1]. As shown in Figure 2D, L-arginine-AP and cerulein+ LPS-AP caused a decrease in pancreatic water content, suggesting pathological atrophy of the pancreas ($P < 0.05$). 9-phenanthrol gradually normalized the abnormal wet weight /dry weight ratio of the pancreas (Figure 2D). Cerulein-AP model mice showed increased pancreatic edema, and 100 $\mu\text{g}/\text{kg}$ of 9-phenanthrol alleviated cerulein-induced pancreatic edema, but there are no signs of significance on Figure 2D. Similarly, level of serum LDH, amylase, and lipase, which are associated with pancreatic acinar cells injury, were also elevated in all three AP models. The application of 9-phenanthrol reduced abnormally elevated serum LDH, amylase and lipase levels ($P < 0.05$, Figures 2E-G).

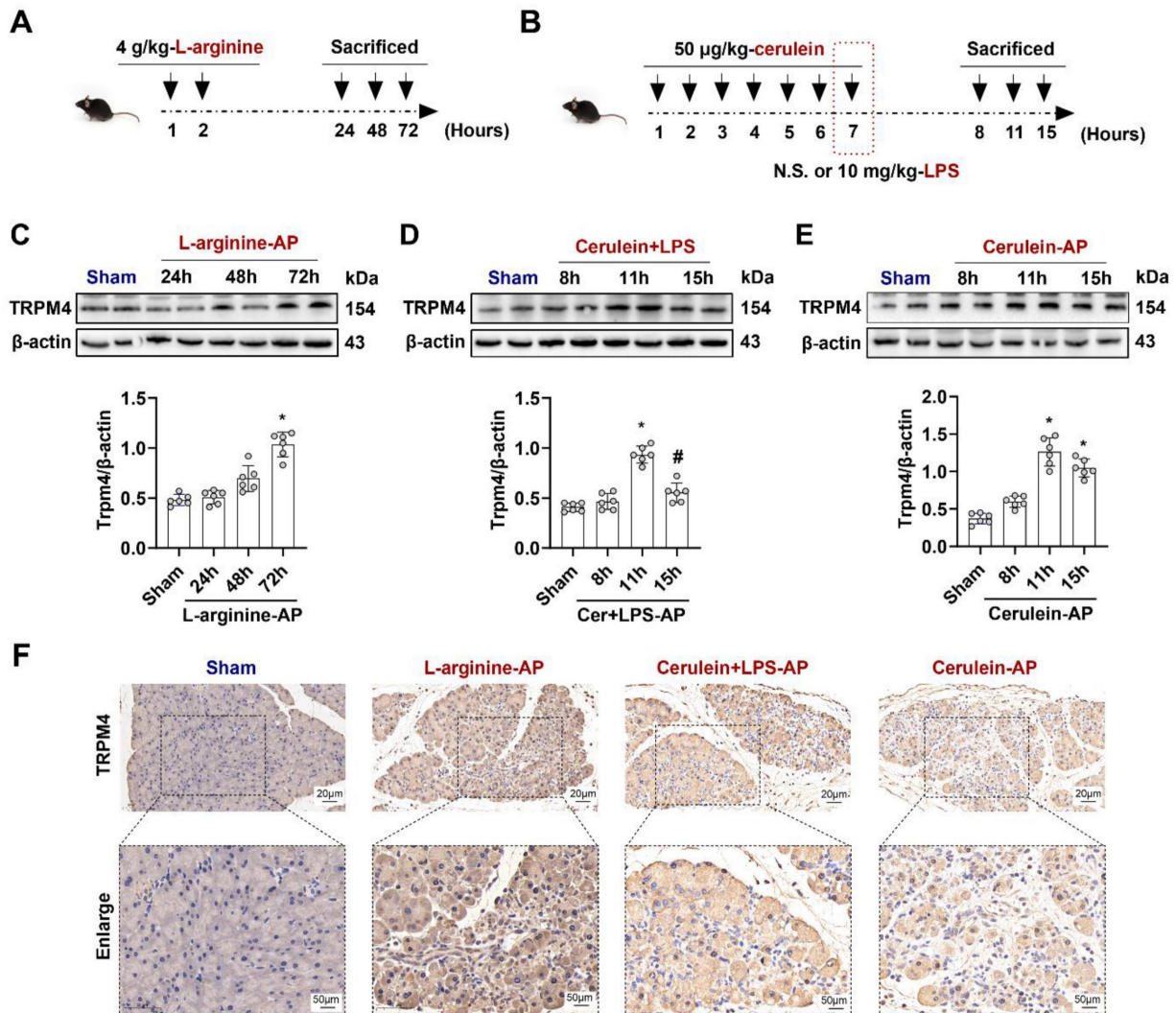


Figure 1. TRPM4 expression levels increased in various AP models. (A) Schematic diagram of L-arginine-AP animal model; **(B)** Schematic diagram of Cerulein+ LPS- or Cerulein-AP animal model; **(C-E)** Western blot analysis the TRPM4 expression level in the pancreas; **(F)** Representative photos of TRPM4 staining of the pancreas (200X or 400X). n = 6, Error bars indicate the SEM; * P < 0.05 vs Sham; # P < 0.05 vs 11h in cerulein + LPS - AP. TRPM4, Transient receptor potential cation channel melastatin 4; AP, acute pancreatitis; LPS, lipopolysaccharide; N.S., normal saline.

The expression of RIP-3, a necrosis-related protein, upregulated in pancreatic tissues of multiple AP models and downregulated after 9-phenanthrol administration (Figures 2H-I). The protective effect of TRPM4 inhibition against apoptosis in pancreatic tissues of AP mice was confirmed by TUNEL staining ($P < 0.05$, Figures 2J-K). Similarly, the expression level of apoptosis-related proteins, i.e., BAX and cleaved caspase-3, which was highly expressed in this AP models, was downregulated after the intraperitoneal injection of 100 µg/kg 9-phenanthrol (Figure 2L).

To further evaluate the protective ability of 9-phenanthrol against AP, a 5-day survival experiment was performed. As shown in Figure 2M, among the 20 L-arginine-induced AP model mice, 7 died on the first day (3 died within 12 h after the procedure). Five died successively over the next 1-2 days. At the end of the experiment (day 5), 12 of the 20

mice had died, resulting in a survival rate of 40%. After treatment with 50 µg/kg 9-phenanthrol, 9 of 18 L-arginine-induced AP model mice died within 2 days; the survival rate of the mice was 50% at the end of the experiment ($P > 0.05$). However, 100 µg/kg 9-phenanthrol increased the survival rate of L-arginine-AP model mice to almost 78% ($P < 0.05$). Similarly, 100 µg/kg 9-phenanthrol increased the survival rate of cerulein+ LPS-induced AP model mice from approximately 50% to more than 80% ($P < 0.05$, Figure 2N). Cerulein-induced AP only caused the death of one experimental animal (Within day 1), and no death was observed after the application of 9-phenanthrol ($P > 0.05$, Figure 2O). These results suggest that cerulein-AP is a mild and self-limiting disease and that the damage only manifests at the organ level, with little systemic effect.

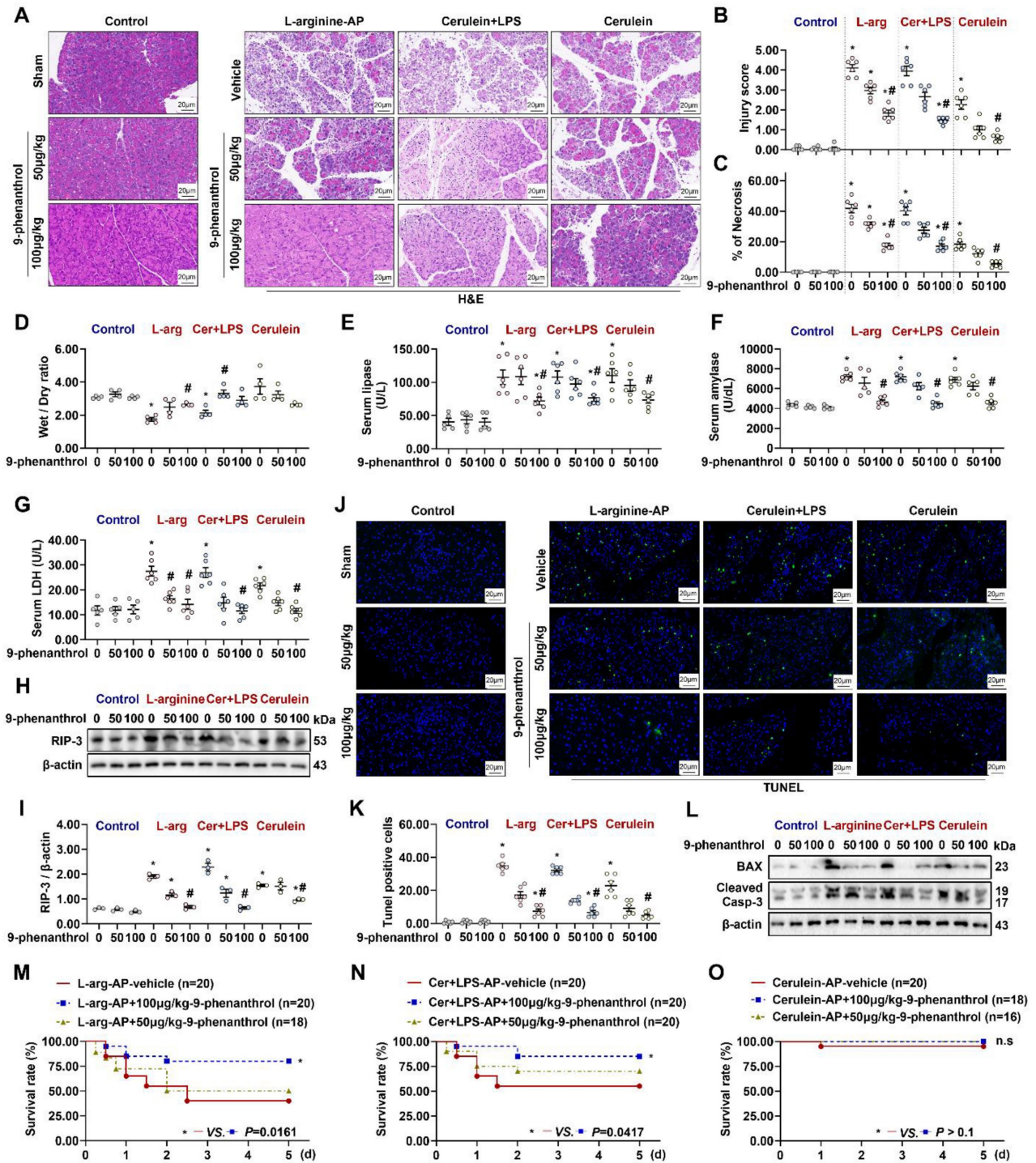


Figure 2. 9-phenanthrol administration was protective in experimental AP. (A) Representative images of H&E staining of the pancreas (200X); (B) Pancreatic injury scores; (C) Percentages of necrotic areas; (D) Pancreatic Wet/Dry ratio; (E) Serum lipase levels; (F) Serum amylase levels; (G) Serum LDH levels; (H-I) Western blot analysis and quantitative of the RIP3 expression level in the pancreas; (J) Representative images of TUNEL staining (200X); (K) Quantitative of TUNEL staining; (L) Western blot analysis of the BAX and Cleaved Caspase-3 expression level in the pancreas; (M) 5-day survival of L-arginine-AP mice; (N) 5-day survival of Cerulein + LPS-AP mice; (O) 5-day survival of Cerulein-AP mice. n = 3-20. Error bars indicate the SEM; * P < 0.05 vs Sham; # P < 0.05 vs Vehicle. RIP3, receptor-interacting protein kinase 3; LDH, lactate dehydrogenase; TUNEL, TdT-mediated dUTP Nick-End Labeling; AP, acute pancreatitis; LPS, lipopolysaccharide.

Inflammation is another pathological feature of AP [7]. In this study, neutrophils were labeled with LY6G to visually observe the changes in the number of inflammatory cells in pancreas. As shown in Figures S2A-B, the intraperitoneal injection of

9-phenanthrol reduced the number of neutrophils in pancreas in AP animal models. Similarly, the elevated levels of IL-6 and TNF-α in the serum of AP mice were also reduced after the application of 9-phenanthrol (Figures S2C-D, P < 0.05).

9-Phenanthrol alleviates mitochondrial dysfunction in experimental AP

Mitochondrial damage plays a central role in the pathogenesis of AP [10, 12]. When AP occurs, mitochondria in pancreatic cells often exhibit swelling, the disappearance of mitochondrial cristae, and even mitochondrial rupture. AP is accompanied by abnormal mitochondrial function protein expression, oxygen free radical metabolism disorder, and endoplasmic reticulum (ER) stress [10, 13]. As shown in Figure 3A, under transmission electron microscopy (TEM), mouse pancreatic cells treated with L-arginine or cerulein+ LPS had abnormal mitochondrial morphology, around which autophagosomes had accumulated. 9-phenanthrol (50 µg/kg) normalized the above mitochondrial morphological abnormalities to a certain extent, while 100 µg/kg 9-phenanthrol basically restored the normal morphology of mitochondria.

As the “energy factory” of the cell, one of the main roles of mitochondria is to produce ATP. Therefore, changes in ATP content directly reflect mitochondrial function. The ATP levels of L-arginine-AP and cerulein+ LPS-AP model mice were reduced to approximately 16% to 17% compared with those of the control mice (Figure 3B). The level was partially restored by treatment with 50 µg/kg 9-phenanthrol ($p > 0.05$) and restored to 80% to 94% of those in control mice by treatment with 100 µg/kg 9-phenanthrol ($p < 0.05$). Normal mitochondrial generation, fusion and mitophagy constitute healthy mitochondrial dynamics. PGC-1 α is crucial regulators of mitochondrial biogenesis [19]. As shown in Figure 3C, western blot analysis showed that PGC-1 α expression level was distinctly downregulated in L-arginine- or cerulein+ LPS- AP model mice. Similarly, Mfn-2 and PINK1, regulators of mitochondrial fusion and mitophagy [20], were also decreased in vehicle-treated AP mice. Administration of 9-phenanthrol restored PGC-1 α , Mfn-2 and PINK1 levels in AP mice. Thus, 9-phenanthrol treatment restored mitochondrial biogenesis and mitophagy in AP.

HSP60 is a mitochondrial protein whose main function is to assist in the proper transport, folding, and assembly of cellular peptides or proteins [21]. HSP60 can be induced by stress, inflammation and immune responses [22, 23]. Immunofluorescence showed that HSP60 expression was increased in AP mice, an effect that was reversed by the administration of 9-phenanthrol (Figures 3D-E). Mitochondrial dysfunction leads to an increase in oxygen free radical production and a protective unfolded protein response (UPR) [11]. DHE fluorescence staining of reactive oxygen species (ROS)

showed that the pancreatic tissue of vehicle treated-AP model mice produced many oxidative stress products (Figures 3F-G), accompanied by a signally decrease in the total antioxidant capacity ($P < 0.05$, Figure 3H). Western blot analysis showed that the ER stress-related proteins, such as phosphor-IRE1 α and GRP78, was also increased in vehicle treated-AP model mice (Figure 3I), suggesting the occurrence of the UPR. The intraperitoneal injection of 9-phenanthrol reduced ROS production, restored the total antioxidant capacity and alleviated ER stress in pancreas of various AP models ($P < 0.05$, Figures 3F-I).

Pancreatic damage was alleviated in experimental AP after *trpm4* knockout

Trpm4 gene knockout (KO) mice were successfully constructed (Figures 4A-B), and we induced AP in this animal to observe the effect of defective TRPM4 expression on AP in mice. As shown in Figures 4C-E, the pancreatic damage in *trpm4*-KO mice was observably alleviated compared with that in wild-type (WT) mice with experimental AP. Additionally, serum amylase and LDH levels decreased to varying degrees in AP mice after *trpm4* KO ($P < 0.05$, Figures 4F-G). TUNEL fluorescence staining and changes in the RIP-3 expression level confirmed that defective TRPM4 expression alleviated pancreatic injury in AP mice ($P < 0.05$, Figures 4H-J). Similarly, pancreatic oxidative stress (Figures 4K-L), mitochondrial damage (Figures 4M-N), ER stress (Figures 4O-P) and inflammation (Figure S3) induced by L-arginine or cerulein+ LPS treatment were also alleviated after *trpm4*-KO in mice.

The overexpression of *trpm4* in AR42J aggravated cerulein-induced cell death and mitochondrial dysfunction

To clarify the role of TRPM4 in pancreatic exocrine acinar cell injury in AP, we overexpressed *trpm4* in AR42J cells (rat pancreatic exocrine cells) by plasmid transfection. As shown in Figure S4, western blot analysis revealed that the transfection of *trpm4* (PI-*Trpm4*) led to an increase in the expression of TRPM4 protein in AR42J. We treated AR42J cells with cerulein+ LPS to mimic pancreatic cell injury in AP *in vitro*.

As shown in Figure 5A, within 24 h after cerulein+ LPS treatment, LDH levels in the supernatant of PI-Vector treated AR42J (control group) gradually increased (Blue line). From 24 h to 48 h, the level of LDH in the supernatant fluctuated slightly, but the level at 48 h was not significantly different from that at 24 h ($P > 0.05$). Transfection with PI-*trpm4* caused cells to release more LDH at 24 h after

cerulein+ LPS treatment than that in control group (Pink line, $P < 0.05$, Figure 5A). An analogical phenomenon was observed for amylase levels in the

cell supernatant (Figure 5B), suggesting that the overexpression of TRPM4 aggravated the destruction of AR42J in the *in vitro* AP model.

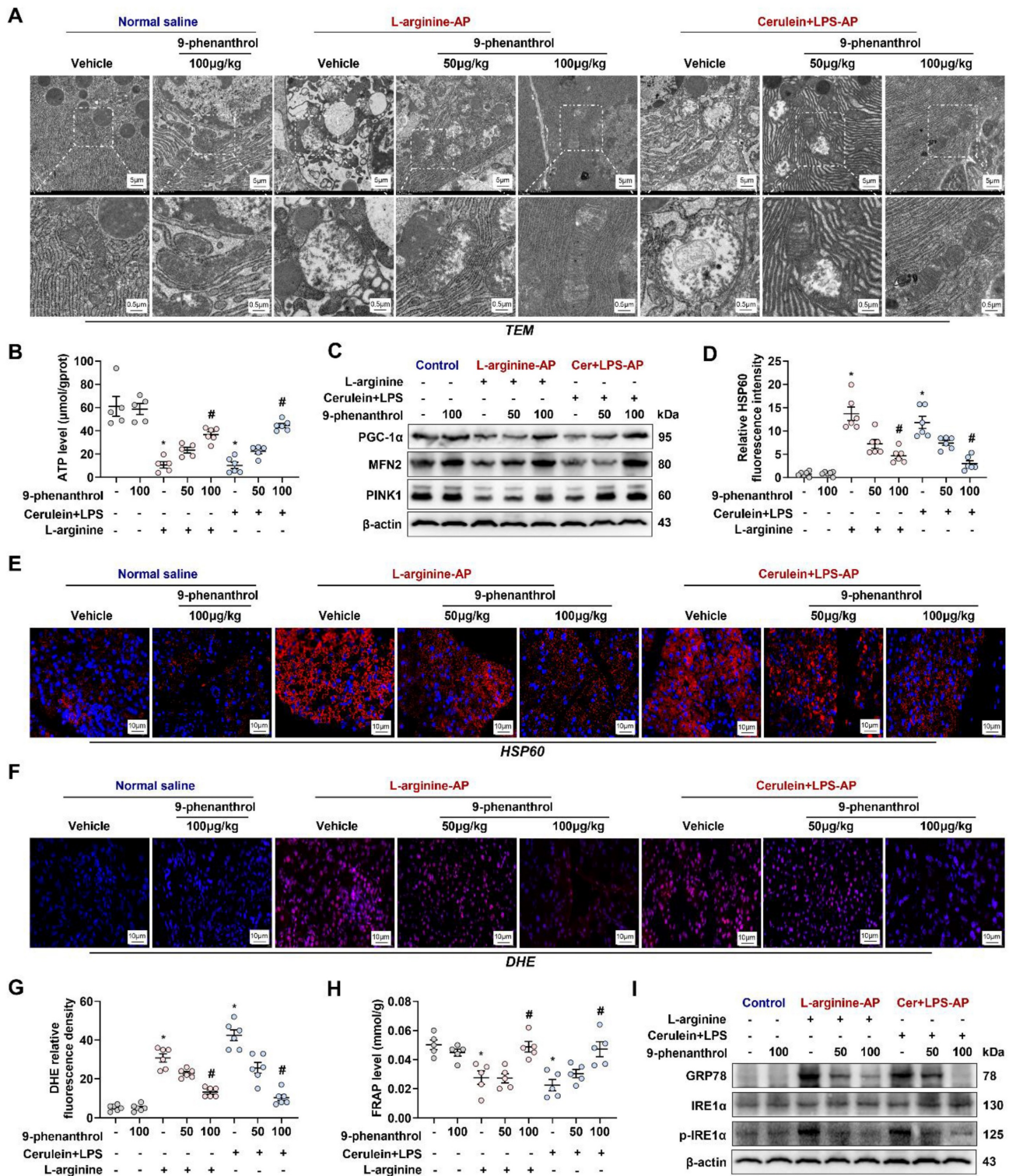


Figure 3. 9-phenanthrol improved mitochondrial function, decreased oxidative stress and alleviates ER stress in experimental AP. (A) Ultrastructural alterations in the pancreas; (B) ATP levels in the pancreas; (C) Western blot analysis of the PGC-1α, Mfn-2 and PINK1 expression level in the pancreas; (D-E) Representative images and relative fluorescence intensity of HSP60 fluorescence staining in the pancreas (600X); (F-G) Representative images and relative fluorescence intensity of DHE staining in the pancreas (600X); (H) FRAP levels in the pancreatic tissue; (I) Western blot analysis of the GRP78, phospho-IRE1α and IRE1α expression level in the pancreas. $n = 6$, Error bars indicate the SEM; * $P < 0.05$ vs Sham group or vs control; # $P < 0.05$ vs Vehicle group. PGC-1α, peroxisome proliferative activated receptor-γ coactivator 1α; PINK1, PTEN induced putative kinase 1; DHE, Dihydroethidium; LPS, lipopolysaccharide; FRAP, Ferric Reducing Antioxidant Power.

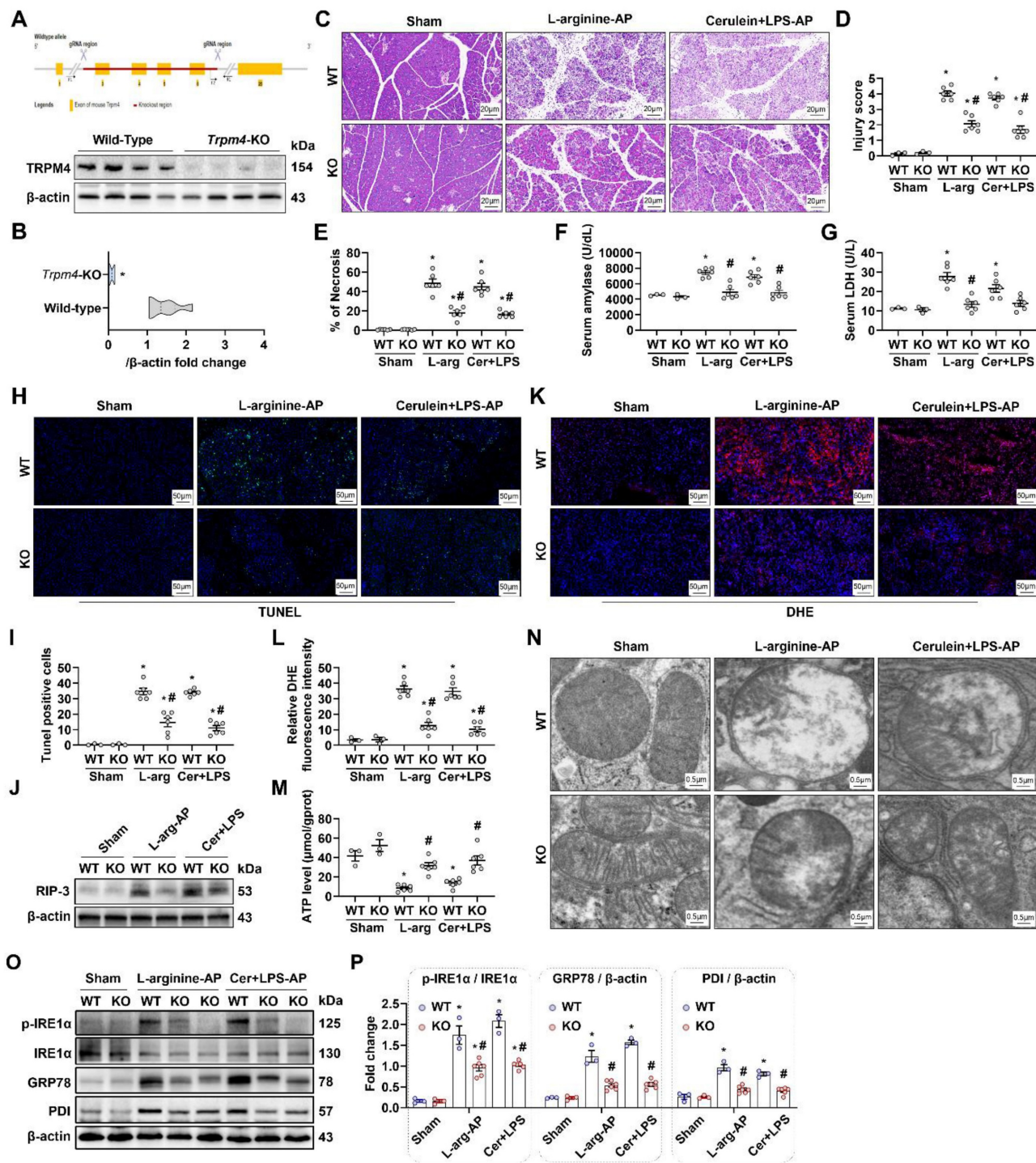


Figure 4. Pancreatic damage was alleviated in experimental AP after *Trpm4*-knockout. (A) Gene editing schematic and western blot analysis of the TRPM4 expression level in the pancreas; (B) Quantitative of the TRPM4 expression level in the pancreas; (C) Representative images of H&E staining of the pancreas (200X); (D) Pancreatic injury scores; (E) Percentages of necrotic areas; (F) Serum amylase levels; (G) Serum LDH levels; (H) Representative images of TUNEL staining (200X); (I) Quantitative of TUNEL staining; (J) Western blot analysis of the RIP3 expression level in the pancreas; (K-L) Representative images and relative fluorescence intensity of DHE staining in the pancreas (600X); (M) ATP levels in the pancreas; (N) Ultrastructural alterations in the pancreas; (O-P) Western blot analysis and quantitates of the GRP78, phosphor-IRE1 α , IRE1 α and PDI expression level in the pancreas. n = 3-6, Error bars indicate the SEM; * P < 0.05 vs Sham; # P < 0.05 vs Vehicle. RIP3, receptor-interacting protein kinase 3; LDH, lactate dehydrogenase; TUNEL, TdT-mediated dUTP Nick-End Labeling; AP, acute pancreatitis; DHE, Dihydroethidium; GRP78, glucose-regulated protein 78; WT, Wild-type; KO, knockout; LPS, lipopolysaccharide.

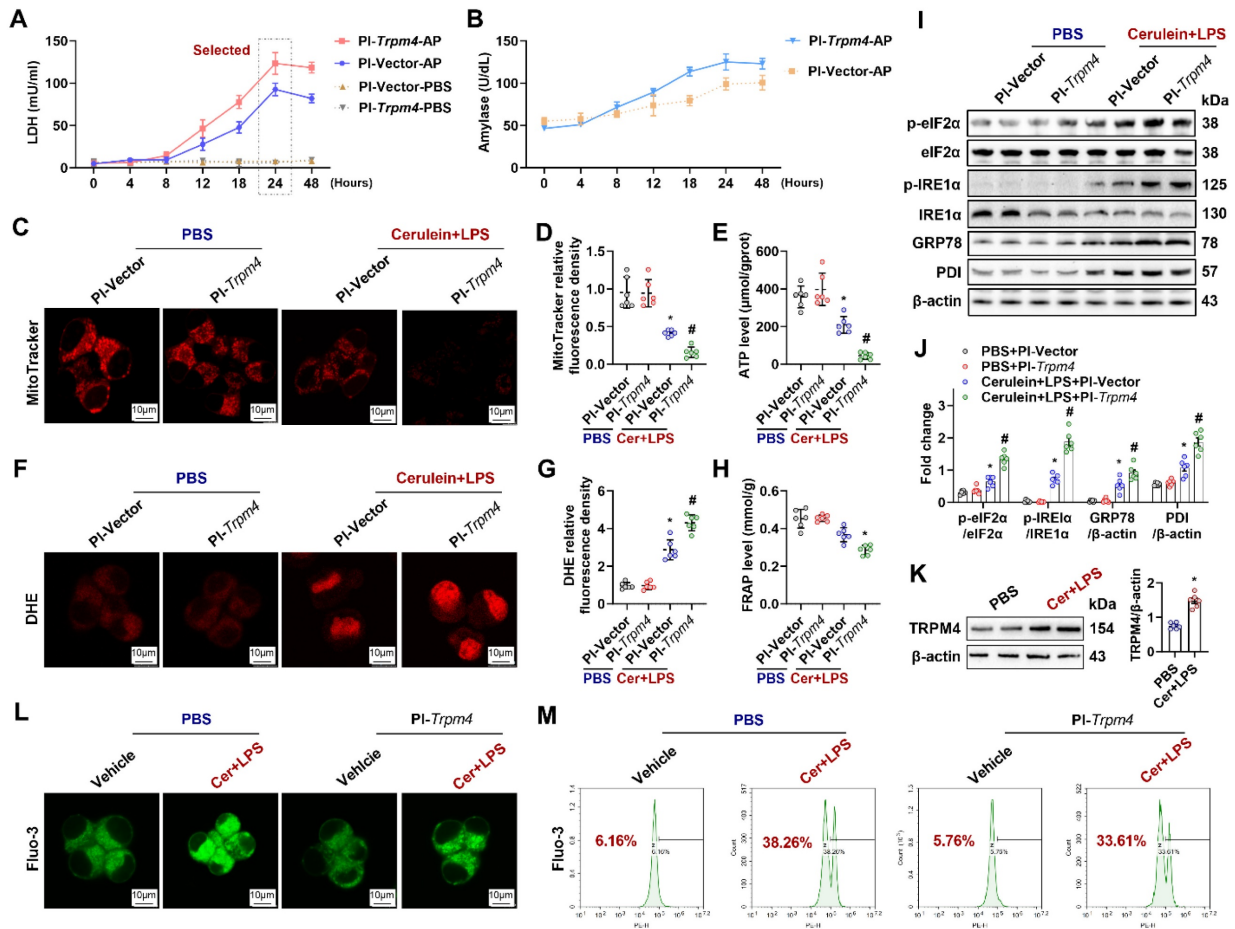


Figure 5. Overexpression of TRPM4 in AR42J aggravated cerulein induced cell death and mitochondrial dysfunction. (A) Supernatant LDH levels; (B) Supernatant amylase levels; (C–E) Representative images and relative fluorescence intensity of Mito-Tracker red (1500X) in AR42J cells; (E) ATP levels in AR42J; (F–G) Representative images and relative fluorescence intensity of DHE (1500X) in AR42J cells; (H) FRAP levels in AR42J; (I–J) Western blot analysis and quantitative of the phosphor-eIF2α, eIF2α, phosphor-IRE1α, IRE1α, GRP78 and PDI expression level in AR42J; (K) Western blot analysis and quantitative of the TRPM4 expression level in AR42J; (L) Representative images of immunofluorescence staining of Fluo-3 (1500X) in AR42J cells; (M) Flow cytometry analysis of Fluo-3 in AR42J cells. n = 6, error bars indicate the SEM; * P < 0.05 vs Sham; # P < 0.05 vs Vehicle. DHE, Dihydroethidium; LPS, lipopolysaccharide; TRPM4, Transient receptor potential cation channel melastatin 4; GRP78, glucose-regulated protein 78; LDH, lactate dehydrogenase; 9-phen, 9-phenanthrol; Cer, Cerulein; FRAP, Ferric ion reducing antioxidant power; Pl, plasmid.

The Mito-Tracker fluorescent dye stains mitochondria in living cells, reflecting the number of functioning mitochondria [24]. As shown in Figures 5C–E, cerulein+ LPS decreased Mito-Tracker fluorescence density and ATP levels in cultured AR42J cells. The overexpression of TRPM4 further decreased Mito-Tracker fluorescence intensity and ATP levels in cerulein+ LPS-treated AR42J cells (P < 0.05). DHE staining and FRAP showed that oxidative stress occurred in the *in vitro* AP models and that oxidative stress was further exacerbated by the overexpression of TRPM4 (Figures 5F–H). The expression of UPR-related proteins showed that ER stress, which occurred in the *in vitro* AP model, was also exacerbated by TRPM4 overexpression (P < 0.05, Figures 5I–J).

Mitochondrial damage and cell death during AP is mainly Ca²⁺-overload dependent [10]. Elevated cytoplasmic Ca²⁺ concentrations in the cytoplasm also activate TRPM4 [17]. In this study, we found that both

the expression level of TRPM4 and the concentration of cytoplasmic Ca²⁺ (Fluo-3 labeled green fluorescence) increased in the *in vitro* AP model (Figures 5K–L). The overexpression of TRPM4 aggravated cerulein+ LPS-induced damage to AR42J but had no significant effect on the concentration of Ca²⁺ in the cytoplasm (Figure 5L). Flow cytometry confirmed this phenomenon, and there was no significant difference in Ca²⁺ concentration between AR42J^{PBS} and AR42J^{PI-Trpm4} cells before or after cerulein+ LPS treatment (Figure 5L–M). These evidences suggest that there may be an entangled relationship between TRPM4 and Ca²⁺ in the occurrence of mitochondrial damage in AP.

9-Phenanthrol inhibited cerulein-induced cell death and mitochondrial damage in AR42J cells

To verify the direct protective effect of TRPM4 inhibition on AR42J, we added different doses of

9-phenanthrol to cerulein+ LPS-treated AR42J cells at 24 h (PI-*trpm4* or PI-*vector*). As shown in Figures 6A-B, with the increase of 9-phenanthrol, the level of amylase and LDH in the supernatant of vehicle- or PI-*Trpm4*- treated AR42J cells gradually decreased. The lowest level was observed in cells treated with 50 ng/ ml and 100 ng/ ml 9-phenanthrol ($P < 0.05$). Mito-Tracker and DHE fluorescence staining showed that 9-phenanthrol relieved cerulein+ LPS induced mitochondrial damage and oxidative stress in AR42J cells (Figures 6C-E). 9-phenanthrol also directly restored mitochondrial PGC-1 α and PINK1 expression (Figure 6F), alleviated ER stress in cerulein+ LPS treated AR42J (Figures 6G-H). The expression level of CHOP increases during ER stress, and CHOP mediating ER stress- related programmed cell death in AP [25]. In this study, 9-phenanthrol decreased the level of CHOP. Figures 6I-M showed that 50 ng/ ml 9-phenanthrol alleviated the aggravation of mitochondrial damage and ER stress caused by TRPM4 overexpression in cerulein+ LPS-treated AR42J.

Quantification of Fluo-3 fluorescence density showed that the TRPM4 inhibitor had no significant effect on the concentration of Ca²⁺ in the cytoplasm of the *in vitro* AP models ($P > 0.05$, Figures 6N-O). These results, combined with those in Figures 5L-M, showed that altering TRPM4 levels in AR42J cells affect mitochondrial dysfunction and cell death without affecting intracellular Ca²⁺ concentration. It is speculated that intracellular Ca²⁺ overload possibly induce mitochondrial dysfunction and AP through TRPM4 mediation. To further elucidate this perspective, we applied Yoda1 to overload Ca²⁺ in mouse pancreatic acinar cells (PACs). Yoda1 is an effective agonist of Piezo1, the activation of which leads to Ca²⁺ overload in acinar cells and induces AP [26].

As illustrated in Figure S5A, the Ca²⁺ concentration in Yoda1-treated mouse PACs increased rapidly, and over time, the levels of LDH in the cell supernatant also gradually increased ($P < 0.05$, Figure S5B). Consistent with our conjecture, the expression level of TRPM4 increased with the continuous increase of intracellular Ca²⁺ (Figure S5C). And the change trend of TRPM4 expression was similar to that of LDH level in cell supernatant. 9-phenanthrol alleviated the aforementioned damage in a dose-dependent manner (Figure S5D) and restored the mitochondrial capacity for ATP production and antioxidation (Figures S5E-F), without affecting Yoda1-induced Ca²⁺ level increase (Figure S5G). These results provide evidence that TRPM4 serves as a mediator in the process by which Ca²⁺ overload disrupts mitochondrial function in acinar cells and promotes cell death.

NMDARs interacts with TRPM4 to induce ER stress and cell death in AR42J

The interaction between NMDARs and TRPM4 plays a momentous role in mitochondrial damage in neurons [18]. To explore the mechanism by which TRPM4 affects pancreatic cells damage, an NMDARs agonist was added to the *in vitro* AP model. As shown in Figure 7A and Figure S6, after the addition of 50 μ M NMDARs agonist (NMDA+), the levels of LDH and amylase in the supernatant of cerulein+ LPS-treated AR42J was increased ($P < 0.05$). 9-Phenanthrol (50 ng/ ml) inhibited the increase in LDH and amylase levels induced by NMDA+ (Figures 7B-C). Analogously, the NMDA+-induced worsening of mitochondrial damage and ER stress in the *in vitro* AP model was attenuated by the administration of 9-phenanthrol (Figures 7D-H). These results imply that the cellular dysfunction induced by NMDARs activation during AP is dependent on the presence of TRPM4.

To test the aforementioned hypothesis, we introduced MK-801+, an NMDARs inhibitor, into the *in vitro* AP model. *Trpm4*-overexpressing AR42J were treated with different concentrations of MK-801 plus cerulein + LPS. As shown in Figures 7I-J, MK-801 at different concentrations had no significant effect on PBS-treated TRPM4-overexpressing AR42J cells. However, with the increase in MK-801 concentration, the aggravation of cell damage caused by TRPM4 overexpression in cerulein+ LPS- treated AR42J cells was gradually alleviated. MK-801 (20 μ M) significantly reduced LDH and amylase levels in the supernatant of AR42J cells ($P < 0.05$). The same protective effect of MK-801 was also observed in mitochondrial and ER stress in AR42J^{PI-*Trpm4*} cells treated with cerulein+ LPS (Figures 7K-O).

We applied MK801 to *in vivo* AP models to validate the results obtained *in vitro*. The intraperitoneal injection of different doses of MK801 alleviated pancreatic damage caused by L-arginine or cerulein + LPS (Figures 8A-C) without affecting TRPM4 expression levels in the pancreas of AP model (Figures S7A-B). In addition, we observed a significant change at a dose of 10 mg/kg MK801 ($P < 0.05$, Figures 8A-C). Similar to the results observed *in vitro*, MK801 alleviated ROS deposition, mitochondrial spoilage and ER stress in AP mice (Figures 8D-H). This evidence confirms that NMDARs interacts with TRPM4 to induce intracellular dysfunction and cell death in AP.

Discussion

Herein, we demonstrated that the expression level of TRPM4 is increased in the pancreatic tissues

of AP mice. We used three animal models of AP, with the aim of conduct preclinical studies that mimic the different pathogeneses of human disease. The study proved that intraperitoneal injection of TRPM4 inhibitors had a protective function on pancreatic injury in various AP model. *In vitro* experiments confirmed that the damage to pancreatic exocrine

acinar cells caused by TRPM4 activation was dependent on the presence of NMDARs. TRPM4, in conjunction with functional NMDARs, mediates mitochondrial dysfunction in acinar cells and exacerbates intracellular oxygen free radical accumulation and ER stress, ultimately leading to cell death (Figure 9).

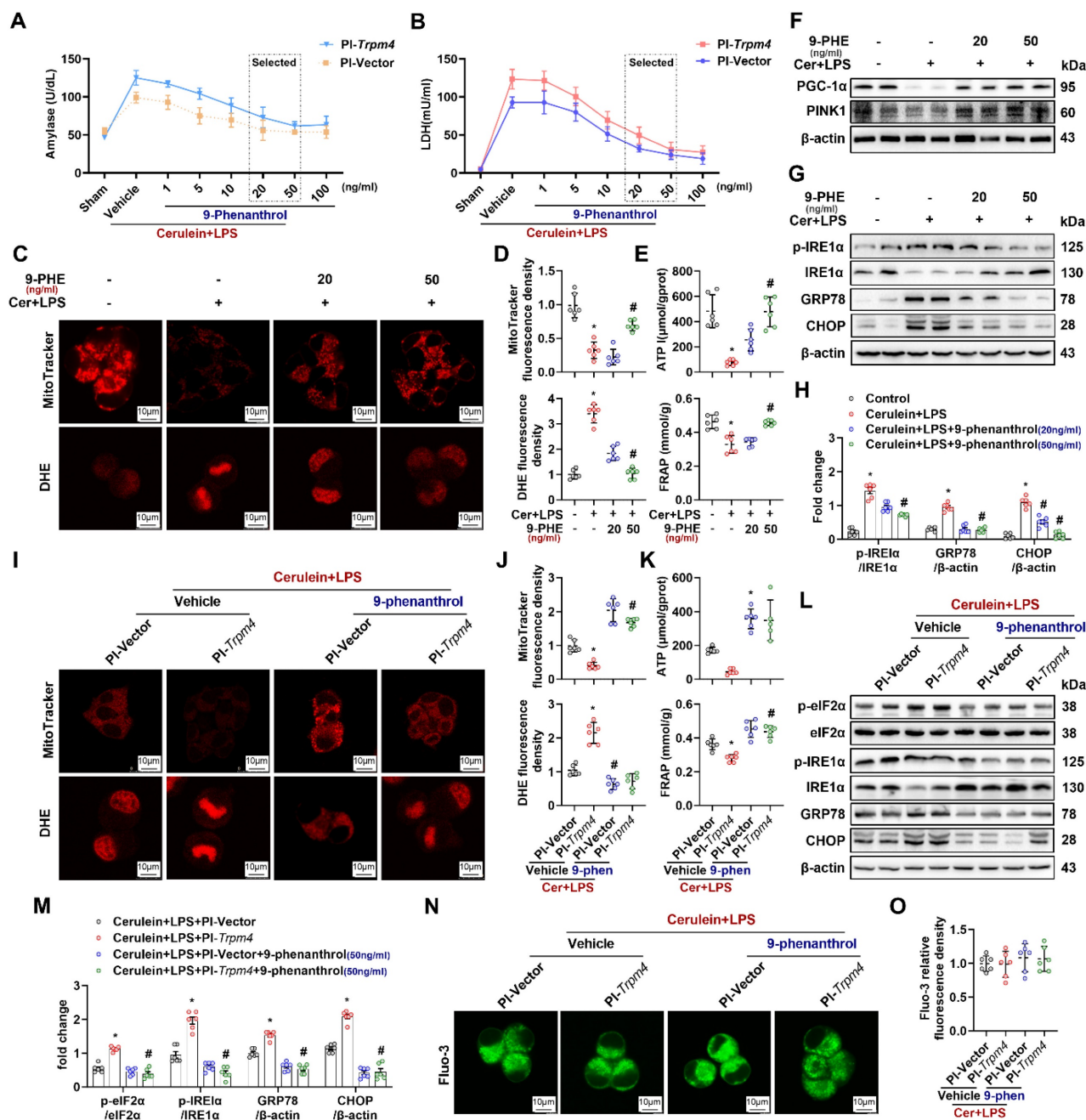


Figure 6. 9-phenanthrol inhibited cerulein induced cell death and mitochondrial dysfunction. (A) Supernatant amylase levels; (B) Supernatant LDH levels; (C) Representative images of Mito-Tracker red and DHE (1500X) in AR42J cells; (D) Relative fluorescence intensity of Mito-Tracker red and DHE in AR42J cells; (E) ATP levels and FRAP levels in AR42J; (F) Western blot analysis of the PGC-1α and PINK1 expression level in AR42J; (G-H) Western blot analysis and quantitative of the phosphor-IRE1α, IRE1α, GRP78 and CHOP expression level in AR42J; (I) Representative images of Mito-Tracker red and DHE (1500X) in AR42J cells; (J) Relative fluorescence intensity of Mito-Tracker red and DHE in AR42J cells; (K) ATP levels and FRAP levels in AR42J; (L-M) Western blot analysis of the phosphor-eIF2α, eIF2α, phosphor-IRE1α, IRE1α, GRP78 and CHOP expression level in AR42J; (N-O) Representative images and relative fluorescence intensity of Fluo-3 (1500X) in AR42J cells. n = 3-4, error bars indicate the SEM; * P < 0.05 vs Sham; # P < 0.05 vs Vehicle. DHE, Dihydroethidium; LPS, lipopolysaccharide; GRP78, glucose-regulated protein 78; LDH, lactate dehydrogenase; CHOP, C/EBP homologous protein; FRAP, Ferric ion reducing antioxidant power; PI, plasmid.

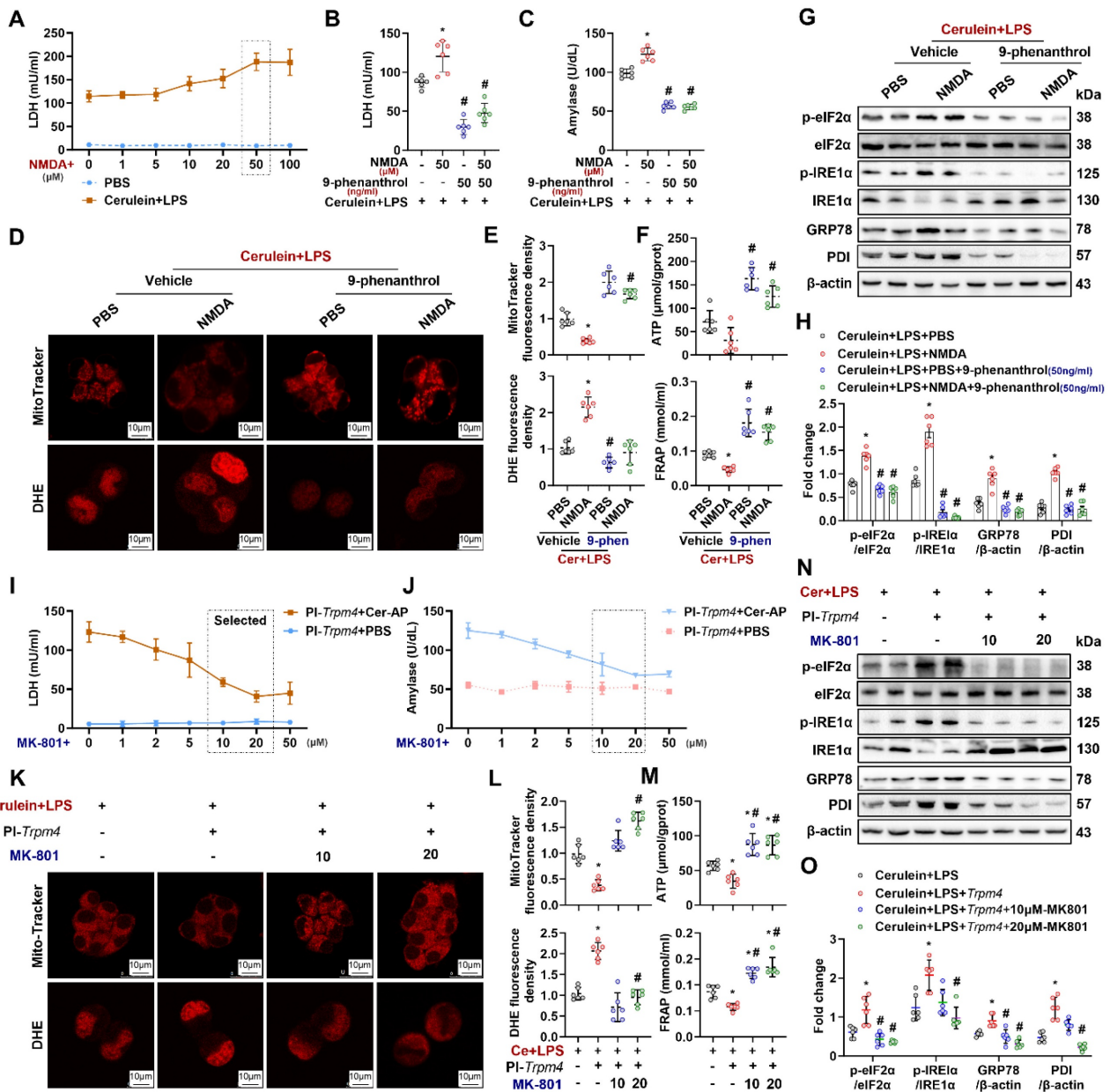


Figure 7. NMDAR interacts with TRPM4 to induce ER stress and cell death in AR42J. (A–B) Supernatant LDH levels; (C) Supernatant amylase levels; (D) Representative images of Mito-Tracker red and DHE (1500X) in AR42J cells; (E) Relative fluorescence intensity of Mito-Tracker red and DHE in AR42J cells; (F) ATP levels and FRAP levels in AR42J; (G–H) Western blot analysis and quantitative of the phosphor-eIF2α, eIF2α, phosphor-IRE1α, IRE1α, GRP78 and PDI expression level in AR42J; (I) Supernatant LDH levels; (J) Supernatant amylase levels; (K) Representative images of Mito-Tracker red and DHE (1500X) in AR42J cells; (L) Relative fluorescence intensity of Mito-Tracker red and DHE in AR42J cells; (M) ATP levels and FRAP levels in AR42J; (N–O) Western blot analysis and quantitative of the phosphor-eIF2α, eIF2α, phosphor-IRE1α, IRE1α, GRP78 and PDI expression levee in AR42J. n = 6, error bars indicate the SEM; * P < 0.05 vs Sham; # P < 0.05 vs Vehicle. DHE, Dihydroethidium; LPS, lipopolysaccharide; GRP78, glucose-regulated protein 78; LDH, lactate dehydrogenase; FRAP, Ferric ion reducing antioxidant power; PI, plasmid; NMDA: N-methyl-d-aspartate.

TRPM4 is a member of the transient receptor potential (TRP) channel family. Previous studies have revealed that the TRPM subfamily is associated with neurodegeneration [27]. TRPM4 is a Ca²⁺-impermeable cationic channel protein that can be activated by intracellular calcium, depolarization, and variation in temperature [28]. TRPM4 is known to be involved in neuropathy, cardiac rhythmopathies, and tumor-related diseases by disrupting mitochondrial homeostasis [15, 29]; however, its role in AP has not

been reported. Currently, it is believed that the key pathogenic mechanism of AP is pancreatic acinar cell mitochondrial damage caused by Ca²⁺ overload [10, 30]. As mentioned above, intracellular Ca²⁺ is involved in the activation of TRPM4, and TRPM4, in turn, is associated with abnormal mitochondrial function. Therefore, it is reasonable to speculate that Ca²⁺ overload in acinar cells caused by different reasons activates TRPM4 and may be participated in the pathogenesis of AP. In this study, both Ca²⁺ and

TRPM4 were elevated in AP models. However, the overexpression of *trpm4* in pancreatic acinar cells and the application of inhibitors to block TRPM4 both affected mitochondrial metabolism without affecting the intracellular Ca^{2+} overload. Changes in TRPM4 appear to be a downstream factor affecting cell death

that should result from high intracellular Ca^{2+} concentration in AP. These findings manifest that elevated Ca^{2+} in the cytoplasm of pancreatic exocrine acinar cells during AP may affect mitochondrial function by activating TRPM4.

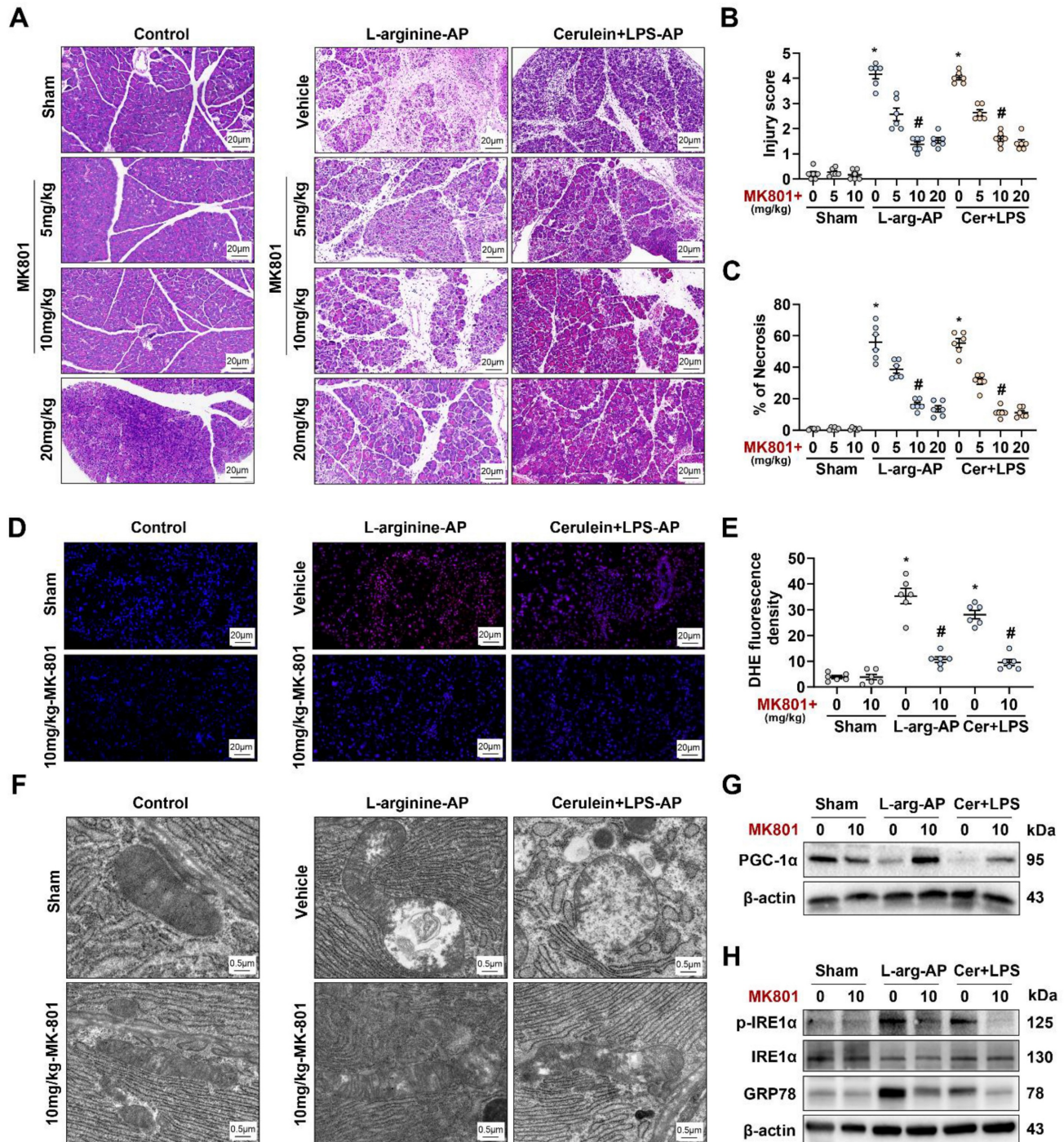


Figure 8. NMDAR interacts with TRPM4 to induce ER stress and pancreatic injury in experimental AP. (A) Representative photos of H&E staining of the pancreas (200X); (B) Pancreatic injury scores; (C) Percentages of necrotic areas; (D-E) Representative images and relative fluorescence intensity of DHE staining in the pancreas (400X); (F) Ultrastructural alterations in the pancreas; (G) Western blot analysis of the PGC-1 α expression level in the pancreas; (H) Western blot analysis of the GRP78, phosphor-IRE1 α and IRE1 α expression level in the pancreas. n = 3-6, error bars indicate the SEM; * P < 0.05 vs Sham; # P < 0.05 vs Vehicle. AP, acute pancreatitis; GRP78, glucose-regulated protein 78; LPS, lipopolysaccharide.

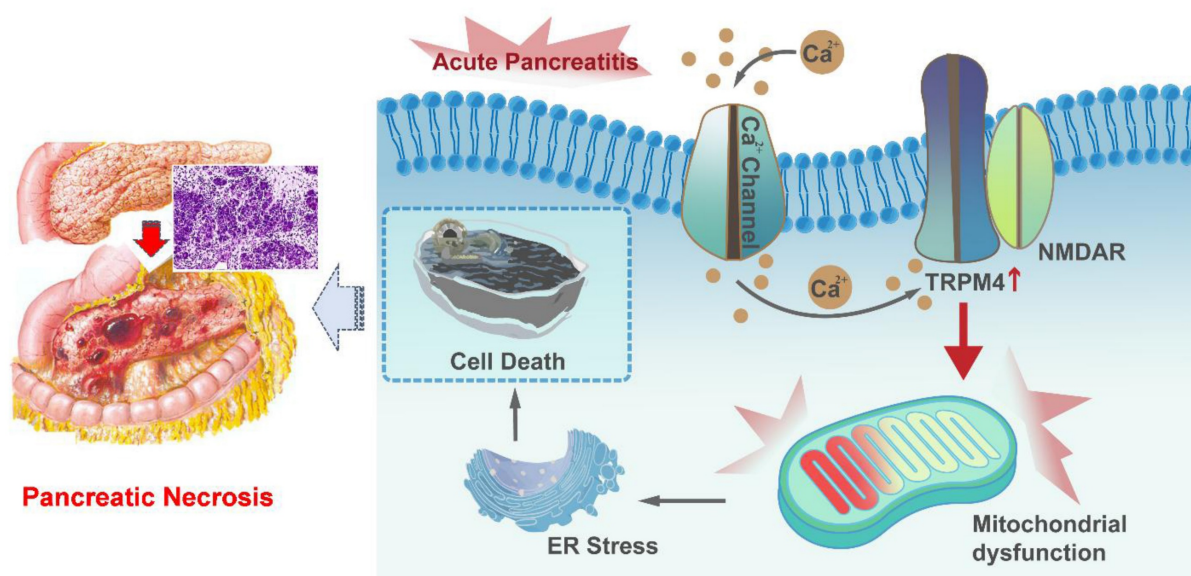


Figure 9. Graphical abstract. When AP occurs, Ca^{2+} overload leads to ER stress and cell death through TRPM4/NMDARs-mediated mitochondrial dysfunction in pancreatic exocrine acinar cells.

Ca^{2+} overload in acinar cells of AP results from multiple factors. Impaired endoplasmic reticulum Ca^{2+} handling and abnormal activation of plasma membrane ion channels, triggered by inflammation and oxidative stress, are key contributors [10]. The role of NMDA receptors in this process is emerging but not fully clear. Pancreatic injury may release glutamate, activating NMDA receptors on acinar cells and promoting Ca^{2+} influx [31]. NMDA receptor activation could also dysregulate other Ca^{2+} - handling proteins, worsening Ca^{2+} dyshomeostasis [32]. However, the involvement of other glutamate receptor subtypes and interactions with other Ca^{2+} - regulating pathways complicate the picture. Future research using selective NMDA receptor antagonists or genetic models is needed to precisely define NMDA receptors' contribution to Ca^{2+} overload, which could reveal new therapeutic targets for AP.

Members of the TRPM family are not only Ca^{2+} -activated cation receptors but also sense temperature changes and produce corresponding functional changes [33]. Our recent work showed that the expression of cold-inducible RNA-binding protein (CIRBP), a temperature-sensitive protein, was increased in AP. Inhibiting the expression of extracellular CIRBP by different means helps to decrease the severity of AP [34]. Therefore, we wondered whether the aggravation of AP induced by CIRBP was also achieved through TRPM4 activation. Because of this low-temperature dependent activation property of TRPM4, it may be a key target for exogenous CIRBP-induced mitochondrial dysfunction of pancreatic acinar cells. Of course, this hypothesis remains to be explored further.

NMDA receptors (NMDARs), a subtype of ionogenic glutamate receptors, are heteromers composed of multiple subunits and are mainly distributed in the central nervous system [35]. Recent evidence shows that NMDARs are not only widely distributed in tissues such as kidney, pancreas, liver and blood vessels but also participate in the maintenance of normal physiological functions of these organs and tissues [36-40]. TRPM4 can physically interact with NMDARs and form the NMDARs/TRPM4 complex, which is involved in mediating neuronal mitochondrial disorder, leading to cell death [18]. Han et al. also found that the NMDARs inhibitor MK801 suppressed LPS-induced mitochondrial damage and apoptosis in endothelial cells [41], suggesting that the presence of NMDARs is involved in the regulation of cellular mitochondrial homeostasis and participated in the destruction of cells caused by damaging factors. In this study, we showed that the activation of TRPM4 resulted in abnormal mitochondrial function and increased cell death in AP. This effect of TRPM4 also appears to be NMDARs dependent. As the NMDARs inhibitor MK-801 inhibited mitochondrial damage aggravated by *trpm4* overexpression in the *in vitro* AP model. Furthermore, 9-phenanthrol, an inhibitor of TRPM4, rescues mitochondrial function and cell death exacerbated by NMDARs agonists, indicating that both functional TRPM4 and NMDARs in pancreatic exocrine acinar cells is a key link mediating mitochondrial dysfunction during AP.

Moreover, we propose that the interplay between NMDA receptors and TRPM4 channels may involve both physical interactions mediated by

proteins like TwinF (as reported by Yan et al.) and functional coupling, where Ca^{2+} influx via NMDA receptors directly activates TRPM4 through Ca^{2+} /calmodulin-dependent mechanisms in AP. This dual-mode interaction, combining structural association and Ca^{2+} -dependent functional regulation, could synergistically modulate cellular excitability and the function of downstream mitochondria. However, due to the lack of evidence, further studies (e.g., Co-IP assays, Ca^{2+} -binding site mutagenesis and other functional experiments) are needed to dissect their respective contributions.

Mitochondria are the "energy factories" of eukaryotic cells and perform oxidative reactions and produce ATP. The stability of their function and morphology maintains the homeostasis of cells [19, 42]. Mitochondrial dysfunction is a key factor in exocrine cells damage in AP [10, 43]. Abnormal mitochondrial function, such as impaired mitochondrial selective autophagy (otherwise known as mitophagy), reduces the oxidative metabolic capacity of a cell, leading to the accumulation of oxygen free radical products [44] and cause oxidative stress [45]. Non-hypoxic induction of mitophagy can be modulated by one of the three classical pathways, the PINK1/Parkin pathway, which plays causative roles in neurodegenerative disease [46]. In this study, we found that the expression of mitophagy protein PINK1 was down-regulated during AP, indicating that AP caused abnormalities in the catabolic process of autophagosome - lysosome to mitochondrial degradation products, including oxygen free radical products. The imbalance of redox process in the cell in turn increases the burden of mitochondria, and then a series of organelle dysfunction occurs. At present, it has been confirmed that ferroptosis is often caused by abnormal mitophagy and the oxidative stress. The combination of these injury factors resulted in irreversible damage of acinar cells during AP, which aggravated tissue destruction [47, 48]. We have demonstrated in both *in vivo* and *in vitro* that inhibition of TRPM4 restores the expression of mitophagy protein PINK1, suggesting that TRPM4-mediated mitochondrial dysfunction is partly caused by affecting its normal autophagy process.

As "energy factories", the decrease in energy production capacity of mitochondria further affects the function of other organelles in the cell, induces ER stress, and reduces the ability of the ER to properly fold proteins. These abnormal functions promote the occurrence of impaired intracellular autophagy (otherwise known as macrophagy), aggravate lipid metabolism disorders in acinar cells, give rise to the expression of apoptosis-related proteins, and ultimately lead to cell death [10, 11]. TRPM4 is

involved in mitochondrial damage and oxidative stress in cardiomyocytes [49], its role in other organelles injury of AP has not been discussed. In this study, the application of 9-phenanthrol to antagonize TRPM4 alleviated the increased mitochondrial damage in both *in vivo* and *in vitro* AP models. And this protective effect of 9-phenanthrol appears to be generated by restoring normal mitochondrial biogenesis and fusion, such as the restoration of PGC-1 α and Mfn-2 expression. By saving mitochondrial functional proteins, the core function of mitochondria - the ability to produce ATP for cells - was also improved. And then, the high expression of the ER stress-related protein CHOP, which mediates apoptosis, decreased after TRPM4 inhibition. Glucose-regulated protein 78 (GRP78) is a hallmark chaperone induced by ER stress. It is vital for protein folding and assembly in the ER and regulation of ER stress initiation mediators, was also decreased after TRPM4 inhibition. The saved endoplasmic reticulum retains the ability to process proteins, promoting the rehabilitation of cell function. The remission of necrosis and inflammation showed that 9-phenanthrol not only restored cell function at the microscopic level but also reduced the damage caused by AP at the macroscopic level. With reference to previous studies on mitochondrial damage in AP, we suggest that these general improvements should be secondary to the protection of mitochondrial function.

There are some limitations to the study. Herein, we discussed the possible role of the NMDARs/TRPM4 complex in acinar cell damage during AP and proposed that the mitochondrial damage in acinar cells caused by intracellular Ca^{2+} overload may be mediated by the NMDAR/TRPM4 complex. However, the specific downstream molecules of NMDAR/TRPM4 that regulate mitochondrial function in exocrine cells during AP is still unknown. The ABCE1 gene is a member of the ATP binding box transporter gene subfamily, and the regulation of ABCE1 alleviates impaired mitochondrial function by affecting mitophagy [50]. In this study, we observed changes in ABCE1 expression when NMDARs/TRPM4 was modulated to affect mitochondrial function (unpublished data). This phenomenon manifests that ABCE1 may be implicated in the regulation of mitochondrial function by NMDAR/TRPM4. Therefore, our future research goals are to explore the role of ABCE1 in mitochondrial damage in pancreatic cells, confirm whether ABCE1 mediates the NMDAR/TRPM4-induced disruption of mitochondrial function during AP, and elucidate the possible molecular signaling pathway through which NMDAR/TRPM4 regulates ABCE1, thereby regulating mitophagy and ultimately

affecting mitochondrial function in AP.

The activation of TRPM4 leading to mitochondrial dysfunction may also be achieved by affecting the mitochondrial membrane potential ($\Delta\Psi_m$). As mentioned before, TRPM4 is a Ca^{2+} -activated cation channel that alters the cell membrane potential by regulating the flow direction of cations. Plasma membrane potential changes may directly interfere with mitochondrial electrochemical gradients via voltage-dependent ion channel crosstalk. Our experiments shows that the expression of ABCE1 changes under the above circumstances, but its role in regulating $\Delta\Psi_m$ remains unvalidated. The potential contribution of TRPM4-induced $\Delta\Psi_m$ disruption warrants mechanistic exploration, particularly regarding ABCE1-mediated trafficking or functional coupling.

Another limitation of this study is regarding the application of inhibitors. While 9-phenanthrol was used here based on prior research, its potential off-target effects highlight a limitation, as 4-chloro-2-[2-(2-chloro-phenoxy)-acetyl-amino]-benzoic acid (CBA) shows more selectivity for TRPM4 and meclofenamate has been validated in animal models [17, 51]. Future studies using these selective inhibitors will help dissociate TRPM4-specific effects from off-target actions, strengthening mechanistic insights into TRPM4-mediated mitochondrial damage.

In conclusion, the results of this study prove that TRPM4 expression in acinar cells mediates mitochondrial damage during AP, contributing to organelle dysfunction and cell death. This involvement of TRPM4 in acinar cell damage may be NMDARs dependent. In addition, the NMDAR/TRPM4 complex may be a key signaling node in intracellular Ca^{2+} overload-induced mitochondrial damage and AP.

Materials and Methods

Animals: Male C57BL/6 J mice (age, 9-10 weeks; weight, 20-22 g) were purchased from Xi'an Huaren Biotechnology Co., LTD and housed in the Experimental Animal Center of Xi'an Jiaotong University. *Trpm4* gene knockout (*trpm4*-KO) mice (Cyagen Biosciences, Inc., Jiangsu, CN) were generated and used in this study, Detailed primer sequences are listed in the supplementary material. Wild-type littermates were used as controls.

In vivo models: Mice were fasted for 8-12 h before the procedure. Arginine-induced AP mice were generated by 2 hourly intraperitoneal injections of 4 g/kg L-arginine (A640158, Aladdin Scientific, CN) [12]. The animals were anesthetized by isoflurane inhalation at 24, 48 or 72 h after the first injection of L-arginine. Blood samples and pancreatic tissues were

collected. In other groups of L-arginine-induced AP model, at 3 h after the first injection of L-arginine, normal saline (vehicle) or 20, 50, 100 $\mu\text{g}/\text{kg}$ 9-phenanthrol (E0028, Selleck, Inc. CN) was administered via intraperitoneal injection. The animals were anesthetized at 72 h after the first injection of L-arginine (i.e., 69 h after 9-phenanthrol treatment).

At 3 h after the first injection of L-arginine, normal saline (vehicle) or 5, 10, 20 mg/kg MK-801 (S2876, Selleck, Inc. CN), a specific NMDA receptor antagonist, was administered by intraperitoneal injection. The animals were anesthetized at 72 h after the first injection of L-arginine (i.e., 69 h after MK-801 treatment). In additional groups of L-arginine-induced AP, survival was monitored for 5 days after vehicle treatment or 9-phenanthrol.

Cerulein + LPS-induced AP mice were generated by 7 hourly intraperitoneal injections of 50 $\mu\text{g}/\text{kg}$ cerulein (C6660, Solarbio, CN). 10 mg/kg lipopolysaccharide (LPS) (L8880, Solarbio, CN) was added to the last cerulein injection [13]. The animals were anesthetized at 8, 11 or 15 h after the first injection of cerulein (i.e., 1, 4 or 8 h after the last injection of cerulein). In another group of cerulein + LPS-induced AP mice, at 30 min after the second injection of cerulein, normal saline (vehicle) or 20, 50, 100 $\mu\text{g}/\text{kg}$ 9-phenanthrol was administered. The animals were sacrificed at 11 h after the first injection of cerulein.

At 30 min after the second injection of cerulein, normal saline (vehicle) or 5, 10, 20 mg/kg MK-801 (S2876, Selleck, Inc. CN), a specific NMDA receptor antagonist, was administered via intraperitoneal injection. The animals were sacrificed at 11 h after the first injection of cerulein. In additional groups of cerulein + LPS-induced AP, survival was monitored for 5 days after vehicle treatment or 9-phenanthrol.

Cerulein-induced AP mice were generated by 7 hourly intraperitoneal injections of 50 $\mu\text{g}/\text{kg}$ cerulein (C6660, Solarbio, CN). The animals were anesthetized and sacrificed at 8, 11 or 15 h after the first injection of cerulein. In another group of cerulein-induced AP mice, at 30 min after the second injection of cerulein, 50 or 100 $\mu\text{g}/\text{kg}$ 9-phenanthrol was administered. The animals were sacrificed at 11 h after the first injection of cerulein. In additional groups of cerulein-induced AP, survival was monitored for 5 days after vehicle treatment or 9-phenanthrol.

Cell culture: Pancreatic AR42J cells (CL-0025, Procell, CN) were cultured in AR42J cell specific medium (CM-0025, Procell, CN) in a humidified incubator at 37 °C with 5% CO_2 [13]. Mouse pancreatic acinar cells (PACs) (CP-M226, Procell, CN) were cultured in their specific culture medium (CM-M226,

Procell, CN) within the same conditions. Both cells were implanted into six-well culture plates (5×10^5 /well) or laser confocal plates (5×10^5 /well) for subsequent experiments. Before the experiment, pretreatment with 100 nM dexamethasone (D4902, Sigma-Aldrich, Germany) for 48 h was used to activate AR42J cells to differentiate into acinar-like phenotypes.

In vitro models in AR42J cells and plasmid transfection: AR42J cells were treated with cerulein (100 nmol/L, C6660, Solarbio, CN) and LPS (10 ng/ml, L-8880, Solarbio, CN) for 4, 8, 12, 18, 24 or 48 h. An equal volume of medium was given as a control. A TRPM4-overexpressing plasmid (PI-*trpm4*) and negative control plasmid (PI-vector) were synthesized by Shanghai Genechem Corporation (CN). The plasmid was extracted and transfected according to the manufacturer's instructions.

In another experiment, AR42J cells were treated with 100 nmol/L cerulein (C6660, Solarbio, USA) and 10 ng/ml LPS (L-8880, Solarbio, CN) with or without, 1, 5, 10, 20 50 or 100 ng/ml 9-phenanthrol (E0028, Selleck, Inc. CN) for 24 h. PI-*trpm4* and PI-vector were transfected into the cells following the manufacturer's instructions.

In another experiment, AR42J were incubated in different concentrations of NMDA (1, 5, 10, 20 50 or 100 μ M) (S7072, Selleck, Inc. CN), a specific NMDA receptor agonist, or MK-801 (1, 2, 5, 10 20 or 50 μ M) (S2876, Selleck, Inc. CN), a specific NMDA receptor antagonist, with or without 50 ng/ml 9-phenanthrol. PI-*trpm4* was transfected into the cells following the manufacturer's instructions.

In vitro models in mouse PACs cells: Mouse PACs were re-cultured in Hanks' Balanced Salt Solution (with Ca^{2+} & Mg^{2+}) (C0219, Beyotime, CN) and treated with Yoda1 (50 μ M, S6678, Selleck, CN) for 1, 2, 3, 10, 20 or 30 min [26, 52]. In another experiment, mouse PACs were treated with 50 μ M Yoda1 with or without 20 or 50 ng/ml 9-phenanthrol (E0028, Selleck, Inc. CN) for 30 min. An equal volume of medium was given as a control.

Statistical analysis: Data were analyzed using GraphPad Prism 10.1.2 Software (San Diego, California, USA) and expressed as means \pm standard error (SEM). The t-test or one-way ANOVA and compared using Student Newman Keuls test was used to analyze the differences between groups. Kaplan-Meier curves were used for survival analysis and log-rank testing for difference analysis. A *P*-value < 0.05 represented a significant difference.

The methods for H&E, immunohistochemical and immunofluorescence staining (HSP60); TUNEL, dihydroethidium (DHE), Mito-Tracker and Fluo-3 staining; ATP and FRAP analyses; enzyme-linked

immunosorbent assays (ELISA); flow cytometry (FCM); biochemical detection; transmission Electron Microscopy (TEM) and western blot analysis are provided in the Supplementary Material.

Abbreviations

AP: Acute Pancreatitis; TRPM4: Transient receptor potential cation channel melastatin 4; NMDARs: N-methyl-d-aspartate receptors; ER stress: Endoplasmic Reticulum stress; PI: plasmid; ATP: adenosine triphosphate; MODS: multiple organ dysfunction syndrome; RIP3: receptor-interacting protein kinase 3; LDH: lactate dehydrogenase; ROS: reactive oxygen species; TUNEL: TdT-mediated dUTP Nick-End Labeling; ELISA: Enzyme-linked immunosorbent assay; UPR: unfolded protein response; HSP60: heat shock protein 60; TEM: transmission electron microscope; PGC-1 α : peroxisome proliferative activated receptor- γ coactivator 1 α ; DHE: Dihydroethidium; CHOP: C/EBP homologous protein; FRAP: Ferric Reducing Antioxidant Power; IRE1 α : inositol-requiring enzyme 1 α ; GRP78: glucose-regulated protein 78; LPS: lipopolysaccharide; AR42J: cells of the rat exocrine pancreas; CIRBP: Cold-induced RNA-binding protein; WT: Wild type; KO: knockout; PINK1: PTEN induced putative kinase 1; P/S: penicillin/streptomycin; n.s: non-significant; PACs: Pancreatic acinar cells; FCM: flow cytometry; CBA: 4-chloro-2-[2-(2-chloro-phenoxy)-acetylamino]-benzoic acid.

Supplementary Material

Supplementary materials and methods, figures and table, blot images, report.
<https://www.thno.org/v15p6901s1.pdf>

Acknowledgements

We thank Yuan Lirong and Ke Mengyun for their administrative support for this study.

Funding

This work was supported by grants from the National Natural Science Foundation of China (No. 82100685, 82370659), the Natural Science Foundation of Shaanxi Province (No. 2024JC-YBQN-0876), and Innovation Capability Support Plan of Xi'an Science and Technology Bureau (No. 23YXYJ0097).

Data availability

Data used to support the findings of this study are available from the corresponding author upon request.

Ethical statement

All experiments were performed in accordance with the guidelines of the China Council on Animal Care and Use and approved by the Institutional Animal Care and Use Committee of the Ethics Committee of Xi'an Jiaotong University Health Science Center.

Author contributions

Ren Y and Cui Q acquired and analyzed the data, wrote the paper. Liu W, Liu H, and Wang T participated in data acquirement. Lu H interpreted the data. Lv Y and Wu R designed and supervised the study and revised the paper. All authors have read and agreed with the final manuscript.

Competing Interests

The authors have declared that no competing interest exists.

References

1. Mederos MA, Reber HA, Girgis MD. Acute Pancreatitis: A Review. *JAMA*. 2021; 325: 382-90.
2. Gardner TB. Acute Pancreatitis. *Ann Intern Med*. 2021; 174: ITC17-ITC32.
3. Ke L, Zhou J, Mao W, Chen T, Zhu Y, Pan X, et al. Immune enhancement in patients with predicted severe acute necrotising pancreatitis: a multicentre double-blind randomised controlled trial. *Intensive Care Med*. 2022; 48: 899-909.
4. Wolbrink DRJ, van de Poll MCG, Termorshuizen F, de Keizer NF, van der Horst ICC, Schnabel R, et al. Trends in Early and Late Mortality in Patients With Severe Acute Pancreatitis Admitted to ICUs: A Nationwide Cohort Study. *Crit Care Med*. 2022; 50: 1513-21.
5. Chanda D, Thoudam T, Sinam IS, Lim CW, Kim M, Wang J, et al. Upregulation of the ER γ -VDAC1 axis underlies the molecular pathogenesis of pancreatitis. *Proc Natl Acad Sci U S A*. 2023; 120: e2219644120.
6. Dingreville F, Panthou B, Thivolet C, Ducreux S, Gouriou Y, Pesenti S, et al. Differential Effect of Glucose on ER-Mitochondria Ca²⁺ Exchange Participates in Insulin Secretion and Glucotoxicity-Mediated Dysfunction of beta-Cells. *Diabetes*. 2019; 68: 1778-94.
7. Habtezion A, Gukovskaya AS, Pandolfi SJ. Acute Pancreatitis: A Multifaceted Set of Organelle and Cellular Interactions. *Gastroenterology*. 2019; 156: 1941-50.
8. Shen Y, Wen L, Zhang R, Wei Z, Shi N, Xiong Q, et al. Dihydrodiosgenin protects against experimental acute pancreatitis and associated lung injury through mitochondrial protection and PI3K γ /Akt inhibition. *Br J Pharmacol*. 2018; 175: 1621-36.
9. Hu Z, Wang D, Gong J, Li Y, Ma Z, Luo T, et al. MSCs Deliver Hypoxia-Treated Mitochondria Reprogramming Acinar Metabolism to Alleviate Severe Acute Pancreatitis Injury. *Adv Sci (Weinh)*. 2023; 10: e2207691.
10. Biczko G, Vegh ET, Shalbuva N, Mareninova OA, Elperin J, Lotshaw E, et al. Mitochondrial Dysfunction, Through Impaired Autophagy, Leads to Endoplasmic Reticulum Stress, Deregulated Lipid Metabolism, and Pancreatitis in Animal Models. *Gastroenterology*. 2018; 154: 689-703.
11. Ren Y, Liu W, Zhang J, Bi J, Fan M, Lv Y, et al. MFG-E8 Maintains Cellular Homeostasis by Suppressing Endoplasmic Reticulum Stress in Pancreatic Exocrine Acinar Cells. *Front Cell Dev Biol*. 2021; 9: 803876.
12. Ren Y, Qiu M, Zhang J, Bi J, Wang M, Hu L, et al. Low Serum Irisin Concentration Is Associated with Poor Outcomes in Patients with Acute Pancreatitis, and Irisin Administration Protects Against Experimental Acute Pancreatitis. *Antioxid Redox Signal*. 2019; 31: 771-85.
13. Ren Y, Liu W, Zhang L, Zhang J, Bi J, Wang T, et al. Milk fat globule EGF factor 8 restores mitochondrial function via integrin-mediated activation of the FAK-STAT3 signaling pathway in acute pancreatitis. *Clin Transl Med*. 2021; 11: e295.
14. Gerasimenko JV, Gerasimenko OV. The role of Ca²⁺ signalling in the pathology of exocrine pancreas. *Cell Calcium*. 2023; 112: 102740.
15. Guinamard R, Bouvagnet P, Hof T, Liu H, Simard C, Salle L. TRPM4 in cardiac electrical activity. *Cardiovasc Res*. 2015; 108: 21-30.
16. Kappel S, Ross-Kaschitzka D, Hauert B, Rother K, Peinelt C. p53 alters intracellular Ca²⁺ signaling through regulation of TRPM4. *Cell Calcium*. 2022; 104: 102591.
17. Vandewiele F, Pironet A, Jacobs G, Kecskes M, Wegener J, Kerselaers S, et al. TRPM4 inhibition by meclizemate suppresses Ca²⁺-dependent triggered arrhythmias. *Eur Heart J*. 2022; 43: 4195-207.
18. Yan J, Bengtson CP, Buchthal B, Hagenston AM, Bading H. Coupling of NMDA receptors and TRPM4 guides discovery of unconventional neuroprotectants. *Science*. 2020; 370 (6513): eaay 3302.
19. Jiang S, Teague AM, Tryggstad JB, Chernausk SD. Role of microRNA-130b in placental PGC-1 α /TFAM mitochondrial biogenesis pathway. *Biochem Biophys Res Commun*. 2017; 487: 607-12.
20. Bhatia D, Chung KP, Nakahira K, Patino E, Rice MC, Torres LK, et al. Mitophagy-dependent macrophage reprogramming protects against kidney fibrosis. *JCI Insight*. 2019; 4 (23): e132826.
21. Ghahari N, Shegefti S, Alaei M, Amara A, Telitichenko R, Isnard S, et al. HSP60 controls mitochondrial ATP generation for optimal virus-specific IL-21-producing CD4 and cytotoxic CD8 memory T cell responses. *Commun Biol*. 2024; 7: 1688.
22. Liyanagamage D, Martinus RD. Role of Mitochondrial Stress Protein HSP60 in Diabetes-Induced Neuroinflammation. *Mediators Inflamm*. 2020; 2020: 8073516.
23. Shi Y, Wu Z, Liu S, Zuo D, Niu Y, Qiu Y, et al. Targeting PRMT3 impairs methylation and oligomerization of HSP60 to boost anti-tumor immunity by activating cGAS/STING signaling. *Nat Commun*. 2024; 15: 7930.
24. Samuvel DJ, Li L, Krishnasamy Y, Gooz M, Takemoto K, Woster PM, et al. Mitochondrial depolarization after acute ethanol treatment drives mitophagy in living mice. *Autophagy*. 2022; 18: 2671-85.
25. Suzuki T, Gao J, Ishigaki Y, Kondo K, Sawada S, Izumi T, et al. ER Stress Protein CHOP Mediates Insulin Resistance by Modulating Adipose Tissue Macrophage Polarity. *Cell Rep*. 2017; 18: 2045-57.
26. Romac JM, Shahid RA, Swain SM, Vigna SR, Liddle RA. Piezo1 is a mechanically activated ion channel and mediates pressure induced pancreatitis. *Nat Commun*. 2018; 9: 1715.
27. Ferreira AF, Ulrich H, Feng ZP, Sun HS, Britto LR. Neurodegeneration and glial morphological changes are both prevented by TRPM2 inhibition during the progression of a Parkinson's disease mouse model. *Exp Neurol*. 2024; 377: 114780.
28. Guo J, She J, Zeng W, Chen Q, Bai XC, Jiang Y. Structures of the calcium-activated, non-selective cation channel TRPM4. *Nature*. 2017; 552: 205-9.
29. Borgstrom A, Peinelt C, Stoklosa P. TRPM4 in Cancer-A New Potential Drug Target. *Biomolecules*. 2021; 11 (2):229.
30. Son A, Ahuja M, Schwartz DM, Varga A, Swaim W, Kang N, et al. Ca²⁺ Influx Channel Inhibitor SARAF Protects Mice From Acute Pancreatitis. *Gastroenterology*. 2019; 157: 1660-72 e2.
31. Cochrane VA, Wu Y, Yang Z, ElSheikh A, Dunford J, Kievit P, et al. Leptin modulates pancreatic beta-cell membrane potential through Src kinase-mediated phosphorylation of NMDA receptors. *J Biol Chem*. 2020; 295: 17281-97.
32. Zhong W, Wu A, Berglund K, Gu X, Jiang MQ, Talati J, et al. Pathogenesis of sporadic Alzheimer's disease by deficiency of NMDA receptor subunit GluN3A. *Alzheimers Dement*. 2022; 18: 222-39.
33. Huang Y, Flegert R, Guse AH, Lu W, Du J. A structural overview of the ion channels of the TRPM family. *Cell Calcium*. 2020; 85: 102111.
34. Liu W, Bi J, Ren Y, Chen H, Zhang J, Wang T, et al. Targeting extracellular CIRP with an X-aptamer shows therapeutic potential in acute pancreatitis. *iScience*. 2023; 26: 107043.
35. Bossi S, Pizzamiglio L, Paoletti P. Excitatory GluN1/GluN3A glycine receptors (eGlyRs) in brain signaling. *Trends Neurosci*. 2023; 46: 667-81.
36. Zrzavy T, Endmayr V, Bauer J, Macher S, Mossaheb N, Schwaiger C, et al. Neuropathological Variability within a Spectrum of NMDAR-Encephalitis. *Ann Neurol*. 2021; 90: 725-37.
37. Dumas SJ, Bru-Mercier G, Courboulin A, Quatredeniens M, Rucker-Martin C, Antigny F, et al. NMDA-Type Glutamate Receptor Activation Promotes Vascular Remodeling and Pulmonary Arterial Hypertension. *Circulation*. 2018; 137: 2371-89.
38. Stepanov YV, Golovynska I, Dziubenko NV, Kuznietsova HM, Petriv N, Skrypkina I, et al. NMDA receptor expression during cell transformation process at early stages of liver cancer in rodent models. *Am J Physiol Gastrointest Liver Physiol*. 2022; 322: G142-G53.
39. Hogan-Cann AD, Anderson CM. Physiological Roles of Non-Neuronal NMDA Receptors. *Trends Pharmacol Sci*. 2016; 37: 750-67.
40. Noguera Hurtado H, Gresch A, Dufer M. NMDA receptors - regulatory function and pathophysiological significance for pancreatic beta cells. *Biol Chem*. 2023; 404: 311-24.
41. Han WM, Hao XB, Hong YX, Zhao SS, Chen XC, Wang R, et al. NMDARs antagonist MK801 suppresses LPS-induced apoptosis and mitochondrial dysfunction by regulating subunits of NMDARs via the CaM/CaMKII/ERK pathway. *Cell Death Discov*. 2023; 9: 59.
42. Akbari M, Kirkwood TBL, Bohr VA. Mitochondria in the signaling pathways that control longevity and health span. *Ageing Res Rev*. 2019; 54: 100940.
43. Choi J, Oh TG, Jung HW, Park KY, Shin H, Jo T, et al. Estrogen-Related Receptor gamma Maintains Pancreatic Acinar Cell Function and Identity by Regulating Cellular Metabolism. *Gastroenterology*. 2022; 163: 239-56.
44. Bansal Y, Kuhad A. Mitochondrial Dysfunction in Depression. *Curr Neuropharmacol*. 2016; 14: 610-8.

45. Liu L, Zhang W, Liu T, Tan Y, Chen C, Zhao J, et al. The physiological metabolite alpha-ketoglutarate ameliorates osteoarthritis by regulating mitophagy and oxidative stress. *Redox Biol.* 2023; 62: 102663.
46. Li J, Yang D, Li Z, Zhao M, Wang D, Sun Z, et al. PINK1/Parkin-mediated mitophagy in neurodegenerative diseases. *Ageing Res Rev.* 2023; 84: 101817.
47. Su L, Zhang J, Gomez H, Kellum JA, Peng Z. Mitochondria ROS and mitophagy in acute kidney injury. *Autophagy.* 2023; 19: 401-14.
48. Li J, Jia YC, Ding YX, Bai J, Cao F, Li F. The crosstalk between ferroptosis and mitochondrial dynamic regulatory networks. *Int J Biol Sci.* 2023; 19: 2756-71.
49. Wang C, Chen J, Wang M, Naruse K, Takahashi K. Role of the TRPM4 channel in mitochondrial function, calcium release, and ROS generation in oxidative stress. *Biochem Biophys Res Commun.* 2021; 566: 190-6.
50. Wu Z, Wang Y, Lim J, Liu B, Li Y, Vartak R, et al. Ubiquitination of ABCE1 by NOT4 in Response to Mitochondrial Damage Links Co-translational Quality Control to PINK1-Directed Mitophagy. *Cell Metab.* 2018; 28: 130-44 e7.
51. Malysz J, Maxwell SE, Petkov GV. Differential effects of TRPM4 channel inhibitors on Guinea pig urinary bladder smooth muscle excitability and contractility: Novel 4-chloro-2-[2-(2-chloro-phenoxy)-acetylamino]-benzoic acid (CBA) versus classical 9-phenanthrol. *Pharmacol Res Perspect.* 2022; 10: e00982.
52. Swain SM, Romac JM, Shahid RA, Pandol SJ, Liedtke W, Vigna SR, et al. TRPV4 channel opening mediates pressure-induced pancreatitis initiated by Piezo1 activation. *J Clin Invest.* 2020; 130: 2527-41.